N-isopropyl chitosan. A pH- and thermo-responsive polysaccharide for gel formation

Michela Cok[a], Marco Viola[a], Federica Vecchies[a], Pasquale Sacco[a], Franco Furlani[a], Eleonora Marsich[b], Ivan Donati[a,*]

[a] Department of Life Sciences, University of Trieste, Via Licio Giorgieri 5, 34127 Trieste, Italy
[b] Department of Medical, Surgical and Health Sciences, University of Trieste, Piazza dell'Ospitale, 34127 Trieste, Italy

ARTICLE INFO

Keywords:
N-isopropyl modified chitosan
pH-stimulus
Thermal stimulus
Hydrogel formation
Rheology

ABSTRACT

The present contribution deals with the synthesis and characterization of *N*-isopropyl chitosan in which the introduction of hydrophobic groups leads to an increased flexibility of the polysaccharide backbone. The isopropyl groups extend the solubility of the modified-chitosan samples and render the modified chitosan a pH- and thermo-sensitive system for hydrogel formation. Indeed, upon varying the pH of the system and/or its temperature within a range compatible with biological applications, a non-reversible sol-gel transition occurs, as determined through extended rheological analyses. The modified chitosan samples show a very good biocompatibility as determined through preliminary viability and cell growth experiments.

1. Introduction

Smart polymeric materials are responsive to different stimuli, such as pH, temperature, light, solvent, magnetic field, redox and mechanical stress. When such stimuli lead to a sol-gel transition with the formation of biocompatible three-dimensional structures, their potential application in the field of drug delivery, biosensors, shape memory materials and biomaterials' development strongly attracts the scientific community (Prasad et al., 2018).

Although synthetic polymers have showed responsiveness towards different stimuli (Amaral & Pasparakis, 2017), the need of good biocompatibility, combined with the emerging interest towards the use of renewable resources, drives the development of stimuli-sensitive materials based on natural polymers.

Chitosan is a biopolymer of natural origin derived from chitin – the second most abundant polysaccharide on earth – present in the exoskeleton of Arthropoda, or from the cell walls of fungi such as zygomycetes (Sacco, Furlani et al., 2018; Vårum & Smidsrød, 2004). The term chitosan describes a family of polysaccharides composed of β-1→4 linked D-glucosamine units (deacetylated units, D) interspersed by residual *N*-acetyl-D-glucosamine residues (acetylated units, A) randomly distributed along the polymer chain. The residual acetylation degree for water-soluble chitosan samples ranges between 5 % and 50 % and the polysaccharide is soluble at acidic pH. The fraction of deacetylated units, F_D, determines the net polymer (positive) charge at a given pH value.

Chitosan is of high interest to obtain stimuli sensitive materials. Recent literature reports examples of chitosan based thermosensitive gels (Matanović, Kristl, & Grabnar, 2014). A system composed of chitosan neutralized with β-glycerophosphate was used as a thermosensitive injectable hydrogel for the sustained release of paclitaxel (Ruel-Gariépy et al., 2004). In addition, injectable chitosan/β-glycerophosphate hydrogels have been proposed as thermosensitive systems for bone tissue regeneration (Saravanan, Vimalraj, Thanikaivelan, Banudevi, & Manivasagam, 2019). Graft polymerization of NIPAAm (Poly *N*-isopropylacryl amide) into a water soluble chitosan leads to a thermosensitive hydrogel for Human MSCs (Mesenchimal Stem Cells) differentiation into chondrocytes (Cho et al., 2004). Chemical modification of the polysaccharide backbone alters the physical-chemical, biochemical and technological properties of chitosan. Stimuli sensitive chitosan derivatives are obtained through phosphorylation (Shanmugam, Kathiresan, & Nayak, 2016), quaternarization (Ren, Zhao, Liang, Ma, & Guo, 2017), carboxylation (Shariatinia, 2018; Wang et al., 2012), sulfonation (Dimassi, Tabary, Chai, Blanchemain, & Martel, 2018), *N*-alkylation and acylation. As an example, local delivery of therapeutic drugs was achieved by means of pH-sensitive materials (Krishna Rao, Vijaya Kumar Naidu, Subha, Sairam, & Aminabhavi, 2006; Li, Liu, & Yao, 2002; Ubaid & Murtaza, 2018; Xu et al., 2019; Yong et al., 2019; Zhang, Jin, Li, Zhang, & Wu, 2018; Zhu, Ma, Zhao, Yang, & Li, 2019). Chitosan was also modified with methacrylate

* Corresponding author.
E-mail address: idonati@units.it (I. Donati).

Accepted 18 November 2019

moieties to yield a light sensitive material which was proposed as component of a dental adhesive system (Diolosà et al., 2014). A lactose-derivative of chitosan (CTL, previously indicated as Chitlac) (Donati et al., 2005) combined with boric acid led to the formation of a transiently reticulated system which displayed stiffening upon application of a mechanical stimulus (Furlani et al., 2019).

The synthesis and characterization of a pH- and thermo- responsive system based on a chitosan modified with isopropyl side chains is the focus of the present contribution. The modified chitosan leads to the formation of hydrogels depending on the balance between hydrophobic and hydrophilic features and on the tunable net charge on the polymer backbone.

2. Materials and methods

Chitosan was purchased from ChitiNor AS (Sollidalen, Norway). The composition was determined by means of ^{1}H-NMR and resulted to be: $GlcNH_2$ = 86 % and GlcNAc = 14 % (MW_{RU} = 198.3 g/mol for the hydrochloride form). The intrinsic viscosity ([η]) was determined to be 920 mL/g by means of capillary viscosimetry (Furlani, Sacco, Marsich, Donati, & Paoletti, 2017) and the weight average molecular weight ($\bar{M}_w$) was determined to be 306,000 ± 15,000 (PI = 1.61 ± 0.08) by means of SEC-MALLS analysis (Christensen, Vold, & Vårum, 2008). Picoline-borane complex, deuterated water, sodium nitrite, sodium hydroxide, MTS Cell Counting Kit and LDH (lactate dehydrogenase)-based TOX-7 kit were purchased from Sigma-Aldrich (Chemical Co. USA). Acetone, sodium chloride, acetic acid, hydrochloric acid, ethanol and methanol were purchased from Carlo Erba (Italy). Deionized water was used in all the preparations. DMEM (Dulbecco's Modified Eagle Medium high Glucose) was purchased from Euroclone (France).

2.1. Synthesis of N-isopropyl derivatives of chitosan (iCT)

N-isopropyl derivatives of chitosan (iCT) reported in Table 1 were obtained as follows in hydrochloride form. 11.25 g of chitosan (57 mmol in repeating units), 315 mL of deionized water and 4.05 mL of glacial acetic acid were loaded on a 5 L reactor, heated at 40 °C and mechanically stirred for 30 min. A solution of methanol (45 mL) containing picoline-borane complex (100 mmol) and acetone (see Table 1) was loaded dropwise in the reactor and the mixture was mechanically stirred for 1 h at 40 °C. The slurry was then added of deionized water (45 mL), the temperature was raised to 60 °C and it was mechanically stirred for 3 h. The solution was cooled to room temperature, added of a 150 mL of aqueous HCl solution (0.86 M) and, after 30 min, the product was precipitated by dropwise addition of acetone (1.25 L). The resulting precipitate was extensively rinsed with acetone to remove the water, air dried and vacuum dried over P_2O_5. For all the derivatives synthesized, the final content of water was found to be lower than 8 %.

Table 1
Composition and zero shear viscosity of the iCT samples at different degree of *N*-isopropyl substitution.

Sample	[Acetone]:[Chitosan][a]	$GlcNH_2$	GlcNAc	GlcN-iPr	η_0 (mPa s)[b]
iCT13	0.2	0.73	0.14	0.13	48.2
iCT37	1	0.49	0.14	0.37	44.9
iCT46	1.2	0.40	0.14	0.46	35.8

[a] Molar ratio between acetone and chitosan repeating units.
[b] Zero-shear viscosity of the hydrochloride salts of iCT measured in water at T = 25 °C (total polysaccharide concentration = 1 % (w/V)). $GlcNH_2$, GlcNAc and GlcN-iPr stand for the (fraction of) residual free glucosamine units, the residual *N*-acetyl glucosamine units and the amount of glucosamine units modified with the isopropyl groups, respectively.

2.2. Intrinsic viscosity measurements

Intrinsic Viscosity was measured at 25 °C by means of a Schott-Geräte AVS/G automatic measuring apparatus and an Ubbelohde-type capillary viscometer. A buffer solution composed of 20 mM AcOH/AcNa, pH 4.5, and 100 mM NaCl was used as a solvent (Sacco, Cok, Asaro, Paoletti, & Donati, 2018). The intrinsic viscosity [η] values were determined by analyzing the polymer concentration dependence of the reduced specific viscosity (η_{sp}/c) and of the reduced logarithm of the relative viscosity ($\ln(\eta_{rel})/c$) using the Huggins (Eq. 1) and Kraemer (Eq. 2) equations, respectively:

$$\frac{\eta_{sp}}{c} = [\eta] + k'[\eta]^2 c \quad (1)$$

$$\frac{ln(\eta_{rel})}{c} = [\eta] - k''[\eta]^2 c \quad (2)$$

where k' and k" are the Huggins and Kraemer constants, respectively.

2.3. ^{1}H-NMR

iCT samples were analyzed at 80 °C by means of ^{1}H-NMR spectroscopy carried out on a 400 VNMRS Varian NMR spectrometer operating at 400 MHz. Samples were prepared according to the procedure previously reported (Sacco, Cok et al., 2018; Sacco, Furlani et al., 2018).

2.4. Rheological measurement

Rheological tests for iCT samples were performed under continuous shear conditions to determine the steady viscosity values in the stress (τ) range 0.1–1000 Pa, as well as under oscillatory shear conditions to determine the extension of the linear viscoelasticity regime (stress sweep tests at ν = 1 Hz) and the mechanical spectrum (frequency sweep, τ = 1 Pa, within the linear viscoelastic regime). The complex viscosity (η*), the storage (G') and loss (G") moduli were recorded in the frequency range 0.01–50 Hz. All tests were carried out with the controlled stress rheometer HAAKE MARS III operating typically at T = 25 °C. A glass bell covering the measuring device was used to improve thermal control and limit evaporation. A cone-plate CP60/1° geometry was used for solutions while a shagreened plate-plate apparatus (∅ = 20 mm) was used in the case of hydrogels. In the case of temperature variations, short stress sweep measurements were performed with τ in the range 1 Pa – 10 Pa and a frequency of 1 Hz and the elastic and viscous moduli were recorded at 25 °C, 37 °C and 45 °C, respectively. In the case of temperature sweep, G' and G" were measured upon increasing the temperature in the range 20 °C – 55 °C (ν = 0.1 Hz; τ = 1 Pa; pH = 7.6; polysaccharide concentration = 10 g/L)

2.5. Turbidimetry

Turbidimetric measurements were performed at 600 nm by means of UV–vis spectroscopy using a UV–vis Amersham Biosciences, Mod. Ultraspec 2100 pro. Aqueous solutions of iCT (hydrochloride form) at different polymer concentration were titrated with NaOH to a specific pH value and the total absorbance measured. Similarly, aqueous solutions of iCT at a pH value of 6 (to avoid precipitation due to the pH) containing increasing amounts of methanol were prepared and their total absorbance measured.

2.6. Viability assay

The viability of a NIH-3T3 cell line treated with iCT was evaluated by MTS assay (Promega). 1×10^3 cells/well were plated in a 96 well plate and allowed to adhere overnight. The next day (day 0) a final concentration of 0.2 % of iCT was added to the growth medium (DMEM

High Glucose supplemented with 10 % FBS and 1 % penicillin/streptomycin). At different time points (0, 1, 4, 5, 6 days) MTS assay was performed and absorbance was measured at 450 nm using a TECAN Infinite® 200 PRO NanoQuant spectrophotometer. Six replicates were analyzed for each sample at each time point. Cells cultured in DMEM High Glucose were used as control.

2.7. Lactate dehydrogenase (LDH) assay

The *in vitro* cytotoxicity of iCT was evaluated by an LDH assay on NIH-3T3 cells. 2000 cells were seeded on 96-well plates. After complete adhesion, the medium was changed and fresh one was added to each well. iCT was added to the growth medium at a final concentration of 0.2 %. After 24 h, medium was collected and the LDH assay was performed according to the manufacture's protocol. Cells that were not exposed to the compound were used as control. Six replicates were analyzed for each treatment. Evaluation of cytotoxicity was calculated according to the following formula:

$$LDH\ released\ \%= \frac{A-B}{C-B}X100$$

with A = LDH activity of cells treated with iCT; B = LDH activity of untreated cells and C = LDH activity after total cell lysis at 24 h.

3. Results and discussion

3.1. Synthesis and characterization of iCT

Chitosan has been modified introducing isopropyl side-chains by means of *N*-alkylation using picoline-borane complex as reducing agent. Table 1 reports in detail the composition as determined by ^{1}H-NMR (see Figure S1 in Supporting Information) of the chitosan derivatives obtained and their zero-shear viscosity as calculated using the Cross equation (Sacco et al., 2017).

The decrease in η_0 for the modified samples with respect to the starting chitosan is partially attributed to chain cleavage, given the treatment under acidic conditions during the synthetic procedure. SEC-MALLS measurements allow determining the extent of backbone degradation (Christensen et al., 2008); iCT46 displays a weight average molecular weight of 172,000 ± 13,000 with a PI of 1.62, thus showing a decrease from the initial molecular weight of chitosan (306,000 ± 15,000). Along the same line, the radius of gyration is also decreased from approx. 58.2 nm for chitosan to 36.8 nm for the isopropyl derivative. Focusing on iCT derivatives, the zero-shear viscosity decreases upon increasing the degree of substitution in isopropyl modified samples due to conformational effects.

The use of the Doty-Benoit equation (Benoit & Doty, 1953) (Eq. 3), obtained for wormlike chains in unperturbed conditions, allows determining the persistence length, q, of chitosan and of iCT46:

$$\langle s_z^2\rangle - q^2\left\{\left(N_Z\frac{l}{3q}\right) - 1 + \left(\frac{2q}{N_W l}\right)\left[1-\left(\frac{q}{N_N l}\right)\right]\right\} = 0 \quad (3)$$

were N_N, N_W and N_Z are the number-average, weight-average, and Z-average degree of polymerization, respectively. While ^{1}H-NMR allows calculating the molecular weight of the repeating unit of chitosan and iCT, respectively, the same virtual bond length, l, is used for both samples, i.e. 0.515 nm (Christensen et al., 2008). When Eq. 3 is applied to the case of chitosan, the persistence length is found to be 8.9 nm, thus in reasonable agreement with the value already reported for a chitosan sample of similar weight average molecular weight under the same experimental conditions, i.e. 7.3 nm (Christensen et al., 2008). Similarly, the persistence length of iCT46 is found to be approximately 6.9 nm, thus slightly lower than the unmodified sample. This implies that the introduction of the isopropyl side chain increases the flexibility of the backbone, likely due to the fact that modified glucosamine units act as kinks along the chain altering the regular structuring of the polysaccharide.

From a strict point of view, the Doty-Benoit equation is valid only in theta conditions. The approach proposed by Denkinger & Burchard (1991) based on the correlation between$(\langle s_z\rangle/(2q))^2$ and the weight-average number of the Kuhn segments (N_K) allows evaluating the validity of the results obtained for the persistence length. Figure S2 in Supporting Information shows that the calculated values for chitosan and for iCT are well within the curves re-drawn from literature data (Denkinger & Burchard, 1991).

Intrinsic viscosity [η] measurements provide additional information on the persistence length of the unmodified and *N*-isopropyl modified chitosan samples through the Flory-Fox sphere model ("nondraining" theory) which has been previously used for different polymers (Eq. 4) (Anthonsen, Vårum, & Smidsrød, 1993; Donati et al., 2004; Higashimura, Mulder-Bosman, Reich, Iwasaki, & Robijn, 2000; Navarini et al., 2001).

$$q = \frac{1}{2}\left[\left(\frac{1}{DP\,l}\right)\left(\frac{[\eta]M_w}{\Phi}\right)^{2/3}\right] \quad (4)$$

Where DP is the degree of polymerization. Eq. 4 is strictly valid in the case of random coils of high molecular weight. Although Φ is a function of the spatial distribution form of the chains and it decreases for expanded polymer chains, for the sake of the present calculation it is considered as a constant. In the case of chitosan, the persistence length calculated with Eq. 4 is 7.5 nm while iCT46 displays a slightly lower value, i.e. 5.9 nm. Far from being conclusive, this preliminary analysis shows that the values obtained are in line with the ones reported in the literature, at least for chitosan, and they further show that the introduction of the isopropyl groups slightly increases the flexibility of the polymer backbone. In general terms, the flexibility of the iCT46 compares to the one of a 5 % oxidized chitosan chain (Christensen et al., 2008).

The introduction of isopropyl groups on the chitosan backbone sensibly alters its solubility both as a function of the pH and of the overall polarity of the solvent. In particular, the water-solubility of iCT46 shows a strong dependence from pH and total polysaccharide concentration (Fig. 1a), at variance with the lactose-modified chitosan (Chitlac, CTL) which resulted to be soluble at all values of pH (D'Amelio et al., 2013; Donati, Borgogna, Turello, Casàro, & Paoletti, 2007).

In fact, polymer aggregation, and thus increase in absorbance, occurs at a pH of approx. 12 when the total polymer concentration is set to 1 g/L. However, when the iCT concentration is increased to 5 g/L, polysaccharide aggregation is already detected at pH slightly above 8 while at 10 g/L it occurs at approx. physiological pH (Fig. 1a). Indeed, the higher is the polysaccharide concentration, the lower is the pH value at which polysaccharide aggregation occurs due to chain-chain association driven by hydrophobic interactions. Acidic conditions prevent the latter association due to electrostatic repulsion among the positively charged chains.

^{1}H-NMR titrations allow determining the pKa of the primary and secondary amino groups in iCT46 (see Figure S3 in Supporting Information). In particular, the chemical shift of the proton at C2 in unmodified and isopropyl-modified glucosamine units of iCT is followed upon pH variation. Eq. 5 determines the "apparent" pKa for the two amino groups (Tømmeraas et al., 2002):

$$pKa_{app}(\alpha) = pH + log\left(\frac{1-\alpha}{\alpha}\right) \quad (5)$$

where α is the ionization degree. The "apparent" pKa is related to the dissociation constant of the first acid/base group in the uncharged chain as follows (eq. 6):

$$pKa_{app}(\alpha) = pKa_0 + \Delta pKa(\alpha) \quad (6)$$

where

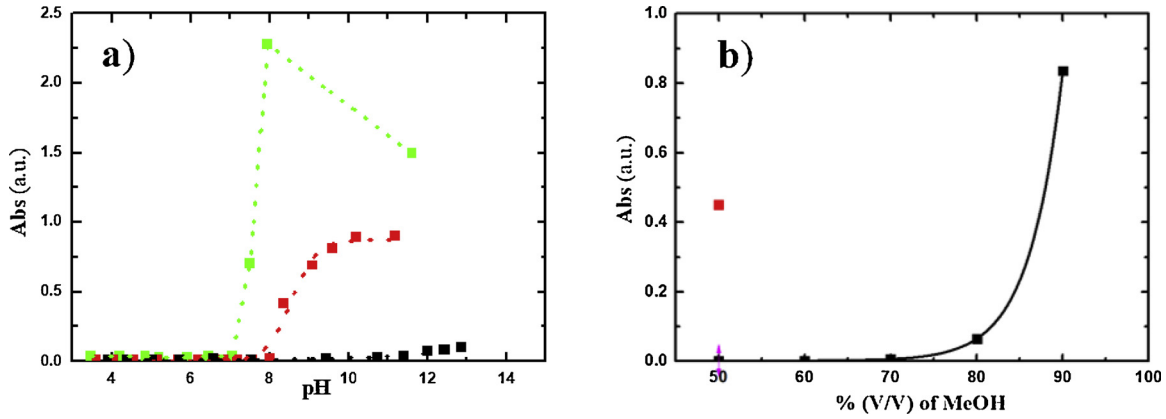

Fig. 1. Effect of the isopropyl groups on solubility of modified chitosan. **a**) Dependence of the absorbance on pH for iCT46 at 1 g/L (■), 5 g/L (■) and 10 g/L (■). **b**) Dependence of the absorbance on the fraction of methanol in iCT solutions (■). Line is drawn to guide the eye. Total polysaccharide concentration 10 g/L. For comparison, the absorbance of a chitosan solution containing 50 % of methanol is reported (■).

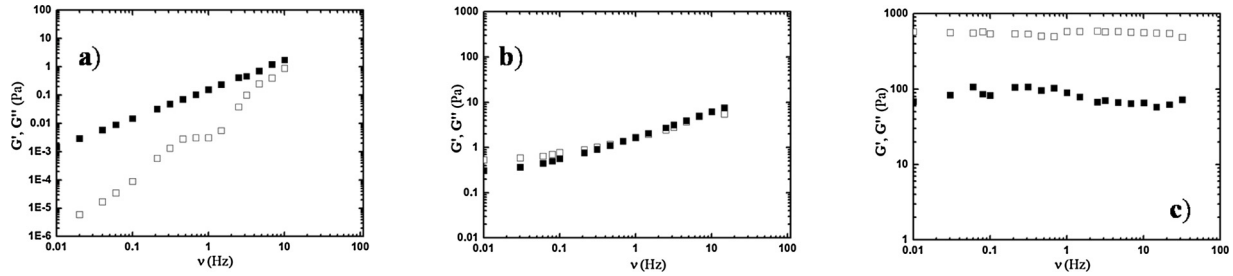

Fig. 2. Effect of pH on sol-gel transition for *N*-isopropyl chitosan (iCT). Dependence of elastic (G', □) and viscous (G", ■) moduli from frequency for iCT46 at 10 g/L at pH 5 (**a**), pH 7.6 (**b**) and pH 8.6 (**c**).

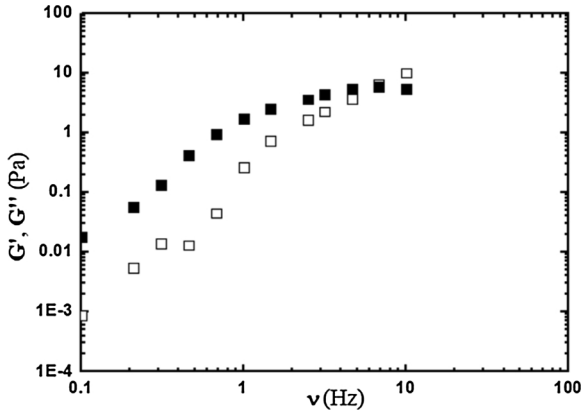

Fig. 3. Rheological effect of the degree of substitution with isopropyl groups on iCT. Dependence of the elastic (G', □) and viscous (G", ■) moduli from frequency for iCT13 at 10 g/L at pH 7.6.

$$\Delta pKa(\alpha) = \frac{1}{n_p 2.303\, RT} \frac{\partial G^{ion}(\alpha)}{\partial \alpha} \tag{7}$$

with n_p the number of polymeric charge units and G^{ion} is the ionic free energy function (Cesàro, Delben, Flaibani, & Paoletti, 1987; Delben, Paoletti, Porasso, & Benegas, 2006).

The Katchalsky plot at α = 0.5 provides the apparent pKa for the primary and secondary amino groups of iCT yielding 6.62 and 7.03, respectively. The $pKa_{app}(\alpha = 0.5)$, i.e. the value of pH at which the stoichiometric concentrations of the charged and of the uncharged species are equal, of the primary amino groups is in very good agreement with the one previously determined for chitosan through the same approach (D'Amelio et al., 2013; Tømmeraas et al., 2002). As expected, the secondary amine shows a slightly higher $pKa_{app}(\alpha = 0.5)$. This is at variance with the $pKa_{app}(\alpha = 0.5)$ for the secondary amine of the lactitol-derivative of chitosan, where a contribution of hydrogen bonding alters the dissociation equilibrium (D'Amelio et al., 2013).

The peculiar solubility of iCT manifests also when water is replaced by a polar solvent such as methanol (Fig. 1b). While chitosan displays a limited solubility when 50 % of methanol is used in the system, iCT46 maintains a complete solubility even at alcohol fraction of 80 % (v/v). It is straightforward to conclude that the presence of isopropyl side chains on chitosan backbone affect its solubility by altering the hydrophobic features of the polymer.

3.2. pH- and thermo-responsive hydrogels formed from iCT

Rheological tests are performed upon varying the pH, temperature and concentration of the isopropyl modified chitosan sample (iCT). Fig. 2(a–c) reports the effect of pH on the mechanical spectrum of iCT46. When the pH of the solution is set to 5, the interchain electrostatic repulsion prevents chain-chain association. Thus, in line with Fig. 1a, the system behaves like a solution, with a viscous response higher than the elastic one. At variance, hydrophobic interactions take place at pH of 9 and the system displays a gel-like behavior, with a marked increase of the elastic response and a G' higher than G" over 3 decades of frequency. The pH 7.6 is a cross-point among the other two conditions explored. Indeed, associations among the isopropyl groups exist, but they are likely not very extended. This results in almost superimposition of the elastic and viscous response.

This is also seen with iCT13 (Fig. 3). In this case, the lower amount of hydrophobic side-chains limits interchain association and the sample at pH 7.6 displays the features of a viscous solution with a cross-over among elastic and viscous moduli only at high frequency values.

Since hydrophobic interactions drive chain-chain association in iCT, the effect of temperature is also explored. Focusing on the single iCT chain, the increase in temperature disrupts the clatrate of water

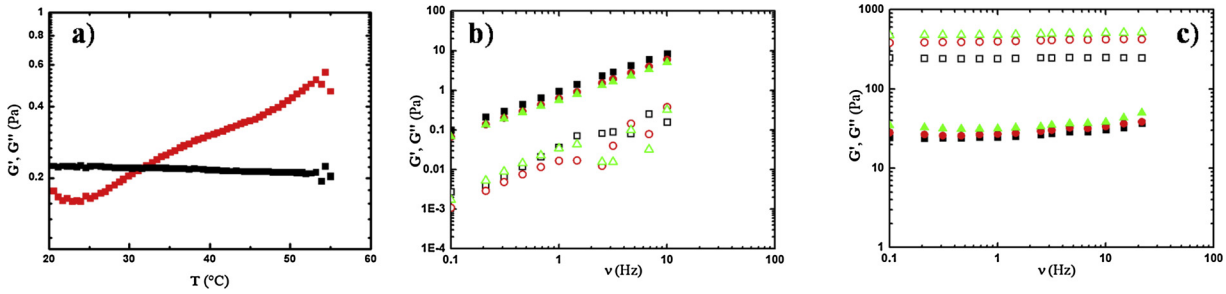

Fig. 4. Effect of pH and temperature on sol-gel transition for iCT. **a**) Dependence of the elastic (G', red) and viscous (G", black) moduli from temperature for iCT46 at a concentration of 10 g/L and pH 7.6. **b**) and **c**) Dependence of the elastic (G', open symbols) and viscous (G", filled symbols) moduli from frequency for iCT46 at 25 °C (black), 37 °C (red) and 45 °C (green) for pH 7.0 (**b**) and 8.2 (**c**). Total polysaccharide concentration = 20 g/L. (For interpretation of the references to colour in this figure legend, the reader is referred to the web version of this article).

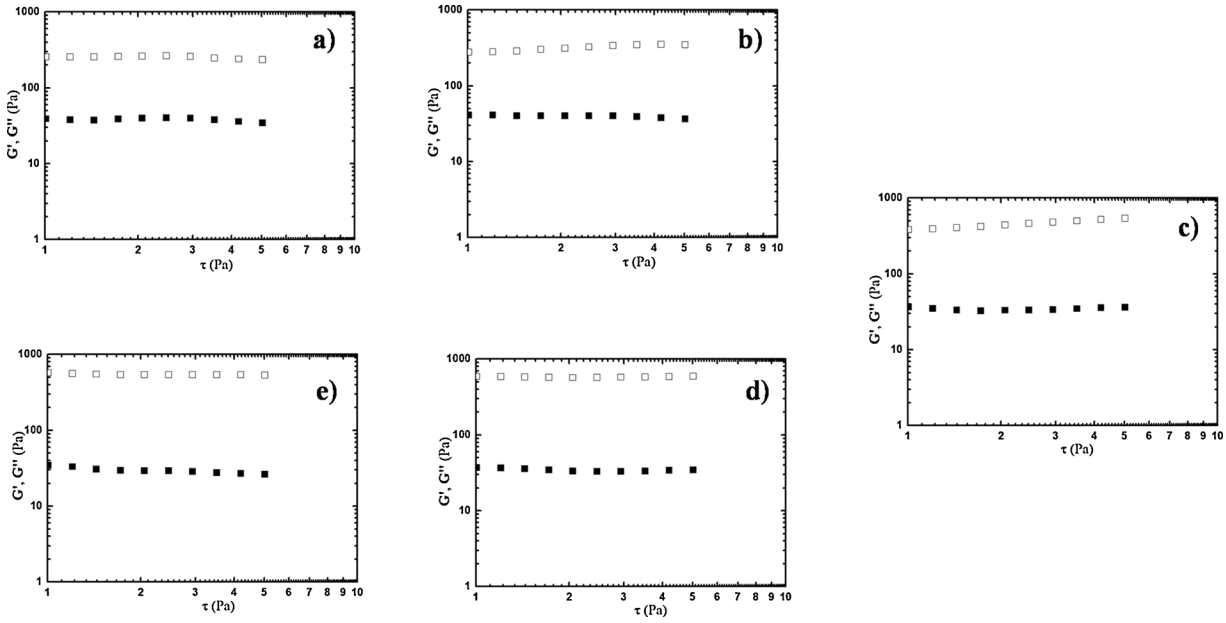

Fig. 5. Effect of temperature ramp on rheology of iCT. Dependence of the elastic (G', □) and viscous (G", ■) moduli from stress for iCT46 at pH 8.2 along the temperature sequence 25 °C (**a**) → 37 °C (**b**) → 45 °C (**c**) → 37 °C (**d**) → 25 °C (**e**). Total polysaccharide concentration = 20 g/L.

molecules around the isopropyl side chain aiding the formation of hydrophobic contacts. A temperature sweep analysis reveals the transition from a liquid-like behavior to a gel-like one for iCT46 with a gel point temperature of approximately 32 °C (Fig. 4a) when the total polymer concentration is set at 10 g/L. This is confirmed by the mechanical response of iCT46 upon increasingthe temperature and using a total polysaccharide concentration of 20 g/L (Fig. 4 b and c).

When the pH is set to 7, the system behaves in a viscous-like manner, with G" higher than G' and the increase in temperature did not affected sensibly the mechanical response (Fig. 4b). In this case, the residual positive charge on the polysaccharide chains prevents the formation of interchain cross-links and this repulsive contribution is not overcome upon increasing the temperature. At variance, hydrophobic chain-chain association takes place at pH of 8.2, leading to a system with an elastic response higher than the viscous one. The application of a temperature ramp strengthens further the chain-chain hydrophobic interactions (Fig. 4c) with three-fold increase in G' upon increasing the temperature from 25 °C to 45 °C. It interesting to note that the additional temperature-induced interchain contacts are stable and not reversed once the temperature is lowered. In fact (Fig. 5 a–e), once a maximum of G' is reached at 45 °C, it remains unaltered upon cooling the system.

3.3. Hydrogel formation through a pH-assisted mechanism and biological properties

The use of pH variation is a very interesting approach for hydrogel formation. Controlling pH-variation, its kinetics and the final value of pH attained is of fundamental importance for biomaterials' applications. To this end, bicarbonate is used as proton-consuming agent and added to the solution containing iCT (Sacco, Furlani, Paoletti, & Donati, 2019). Since the latter is synthesized as hydrochloride salt, the protons released from the amino groups will shift the bicarbonate equilibrium towards the production of CO_2 that, evading from the system, will progressively increase the pH. To test this hypothesis, a 20 g/L iCT solution is treated for 4 h with 80 mM of $NaHCO_3$ and the elastic and viscous moduli are measured at 25 °C and after a temperature ramp (Fig. 6a–e). Short stress sweep measurements reveal that at 25 °C the system behaves like a weak elastic material, with G' slightly higher than G". The temperature of the system is then increased to 37 °C and 45 °C, respectively, and Fig. 6b and c show the increase in the elastic modulus of approx. 2 orders of magnitude. In addition, upon reversing the temperature ramp, i.e. bringing the system from 45 °C to 37 °C and then down to 25 °C, the mechanical performance of the system is preserved.

The use of a proton consuming agent allows obtaining wall-to-wall three-dimensional structures. Indeed, when the resting time after the bicarbonate addition extends to 24 h, a rearrangement of the

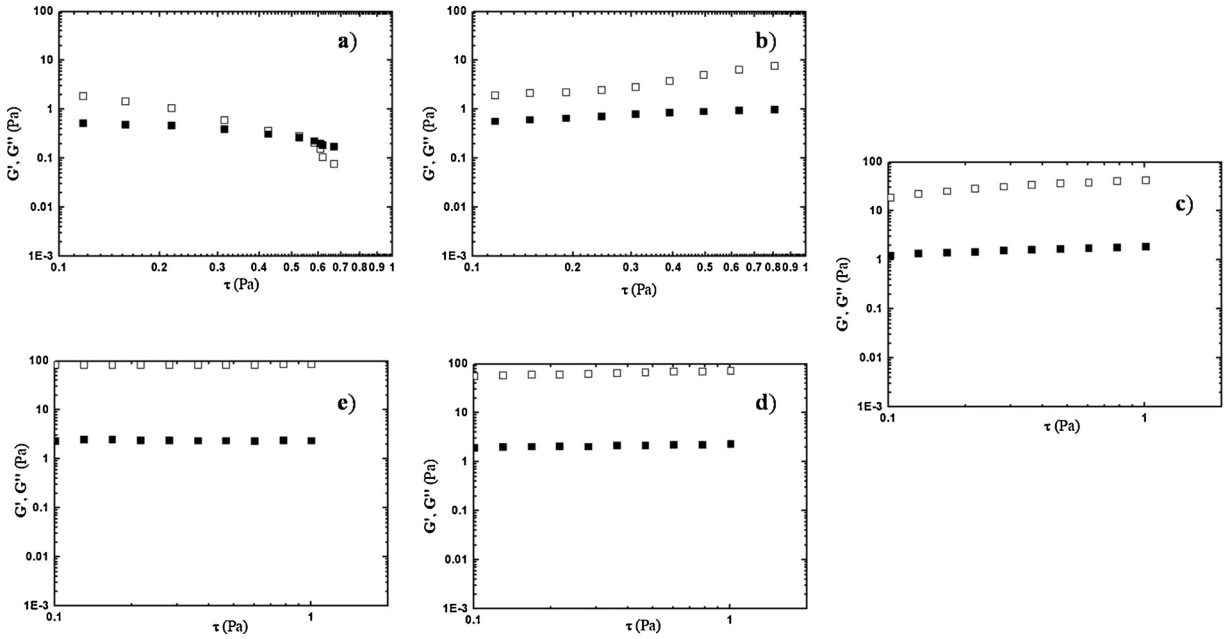

Fig. 6. Sol-gel transition and temperature ramp on iCT hydrogels formed by means of a pH assisted mechanism. Dependence of the elastic (G', □) and viscous (G", ■) moduli from stress for iCT46 treated with $NaHCO_3$ along the temperature sequence 25 °C (**a**) → 37 °C (**b**) → 45 °C (**c**) → 37 °C (**d**) → 25 °C (**e**). Total polysaccharide concentration = 20 g/L.

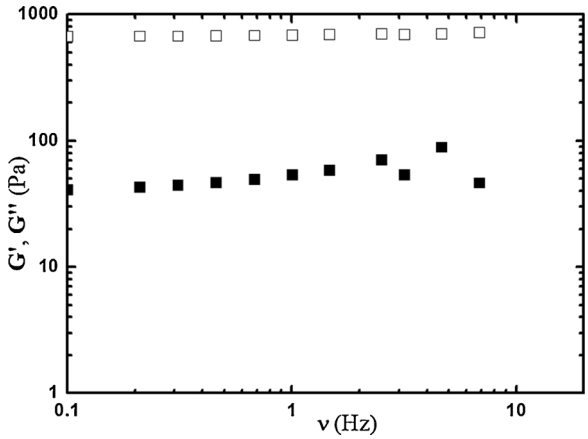

Fig. 7. iCT hydrogels formed though a pH-assisted mechanism. Dependence of the elastic (G', □) and viscous (G", ■) moduli from stress for iCT46 treated with $NaHCO_3$ with a setting time of 24 h. Total polysaccharide concentration = 20 g/L, T = 25 °C.

polysaccharide chains takes place leading to a firm hydrogel (Fig. 7). The elastic modulus is one order of magnitude higher than the viscous one and both are basically independent from the frequency. A comparison between Figs. 6 and 7 shows that G' at 24 h is approx. 6 times higher than that at 4 h after thermal treatment. The effect of temperature ramps is then checked on the hydrogel thus formed by means of short stress sweep measurements (Figure S4 a–e in Supporting Information). Once more, heating leads to further hydrophobic interchain cross-links with a 2.5-fold increase in the elastic response. Although a detailed analysis of the mechanical response of these systems over extended time will be carried out, the results herein reported demonstrate that the iCT system can lead to gel formation with a mechanism triggered and controlled by both pH and temperature.

Measurements of cell viability and growth allow evaluating basic biological properties of iCT (Fig. 8a and b). Both experiments point to a good biocompatibility of the modified material, which does not hamper cell proliferation as, both in the iCT treated cells and in control experiments, cell confluence was reached after 6 days of culture.

4. Conclusions

pH- and thermo-sensitive biocompatible materials based on natural polymers are highly sought by researchers since their potential applications cover a very wide range. Specifically, hydrogel formation triggered by simple and cell-friendly stimuli allows for the use of modified biopolymers in minimally invasive surgery and viscosupplementation for several purposes in tissue engineering. Along this line, the introduction of isopropyl side chains on the backbone of chitosan leads to an interesting modified biopolymer which might represent a novelty in the field. Indeed, the control over the amount of hydrophobic side chains introduced allows tuning the physical-chemical properties of the modified chitosan. Although chain flexibility (persistence length) is only limitedly affected, the solubility of the modified chitosan with respect to pH and amount of non-solvents such as methanol displays notable modifications. This is traced back to the altered hydrophilic/hydrophobic character, which endows the *N*-isopropyl chitosan (iCT) with the ability to form hydrogels when electrostatic chain-chain repulsion is limited. Indeed, pH and temperature act as efficient stimuli to elicit the formation of hydrophobically driven chain-chain associations, which can end in the formation of a wall-to-wall hydrogel. It should be stressed that the sol-gel transition occurs at a pH compatible with the applications in the biomedical field and that, in addition, the increase in temperature up to 45 °C strengthens the formed hydrogel in a non-reversible way. Considered the biocompatibility following to preliminary results, *N*-isopropyl chitosan (iCT) shows an interesting potential role for tissue engineering purposes.

Acknowledgments

Dr. Olav Aarstad is thankfully acknowledged for the SEC-MALLS measurements. This study was supported by the INTERREG V-A Italia-Slovenia 2014-2020 BANDO 1/2016 ASSE 1 – project BioApp 1472551605.

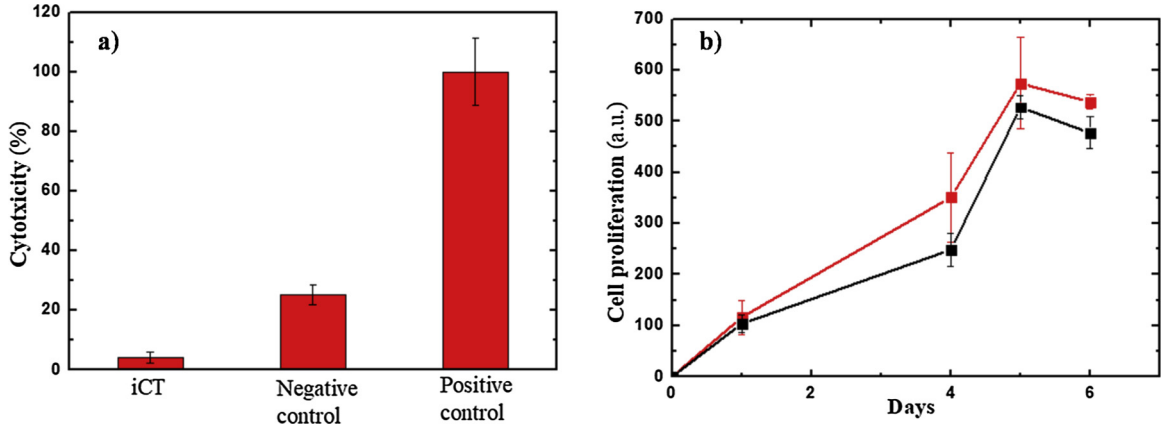

Fig. 8. Lack of biological negative effect of iCT. a) Cytotoxicity, measured as LDH release, by NIH-3T3 cell line treated with iCT46 at a final concentration of 0.2 %. Negative control represents the sole medium while positive control is the LDH released after cell lysis (Triton X). **b**) MTS assay on NIH-3T3 cell line. Cells are treated with iCT46 (red) at a final concentration of 0.2 %. Cells treated with standard growth medium (DMEM) were used as control (black). In both **a**) and **b**), results are reported as mean ± s.d. (n = 6). (For interpretation of the references to colour in this figure legend, the reader is referred to the web version of this article).

Amaral, A. J. R., & Pasparakis, G. (2017). Stimuli responsive self-healing polymers: Gels, elastomers and membranes. *Polymer Chemistry, 8*(42), 6464–6484.

Anthonsen, M. W., Vårum, K. M., & Smidsrød, O. (1993). Solution properties of chitosans: Conformation and chain stiffness of chitosans with different degrees of N-acetylation. *Carbohydrate Polymers, 22*(3), 193–201.

Benoit, H., & Doty, P. (1953). Light scattering from non-gaussian chains. *The Journal of Physical Chemistry, 57*(9), 958–963.

Cesàro, A., Delben, F., Flaibani, A., & Paoletti, S. (1987). Polyelectrolytic effects in carboxylic derivatives of natural polysaccharides. *Carbohydrate Research, 160*, 355–368.

Cho, J. H., Kim, S.-H., Park, K. D., Jung, M. C., Yang, W. I., Han, S. W., ... Lee, J. W. (2004). Chondrogenic differentiation of human mesenchymal stem cells using a thermosensitive poly(N-isopropylacrylamide) and water-soluble chitosan copolymer. *Biomaterials, 25*(26), 5743–5751.

Christensen, B. E., Vold, I. M. N., & Vårum, K. M. (2008). Chain stiffness and extension of chitosans and periodate oxidised chitosans studied by size-exclusion chromatography combined with light scattering and viscosity detectors. *Carbohydrate Polymers, 74*(3), 559–565.

D'Amelio, N., Esteban, C., Coslovi, A., Feruglio, L., Uggeri, F., Villegas, M., ... Donati, I. (2013). Insight into the molecular properties of chitlac, a chitosan derivative for tissue engineering. *The Journal of Physical Chemistry B, 117*(43), 13578–13587.

Delben, F., Paoletti, S., Porasso, R. D., & Benegas, J. C. (2006). Potentiometric titrations of maleic acid copolymers in dilute aqueous solution: Experimental results and theoretical interpretation. *Macromolecular Chemistry and Physics, 207*(24), 2299–2310.

Denkinger, P., & Burchard, W. (1991). Determination of chain stiffness and polydispersity from static light-scattering. *Journal of Polymer Science Part B, Polymer Physics, 29*(5), 589–600.

Dimassi, S., Tabary, N., Chai, F., Blanchemain, N., & Martel, B. (2018). Sulfonated and sulfated chitosan derivatives for biomedical applications: A review. *Carbohydrate Polymers, 202*, 382–396.

Diolosà, M., Donati, I., Turco, G., Cadenaro, M., Di Lenarda, R., Breschi, L., & Paoletti, S. (2014). Use of methacrylate-modified chitosan to increase the durability of dentine bonding systems. *Biomacromolecules, 15*(12), 4606–4613.

Donati, I., Borgogna, M., Turello, E., Casàro, A., & Paoletti, S. (2007). Tuning supramolecular structuring at the nanoscale level: Nonstoichiometric soluble complexes in dilute mixed solutions of alginate and lactose-modified chitosan (Chitlac). *Biomacromolecules, 8*(5), 1471–1479.

Donati, I., Coslovi, A., Gamini, A., Skjåk-Bræk, G., Vetere, A., Campa, C., & Paoletti, S. (2004). Galactose-substituted alginate 2: Conformational aspects. *Biomacromolecules, 5*(1), 186–196.

Donati, I., Stredanska, S., Silvestrini, G., Vetere, A., Marcon, P., Marsich, E., ... Vittur, F. (2005). The aggregation of pig articular chondrocyte and synthesis of extracellular matrix by a lactose-modified chitosan. *Biomaterials, 26*(9), 987–998.

Furlani, F., Sacco, P., Marsich, E., Donati, I., & Paoletti, S. (2017). Highly monodisperse colloidal coacervates based on a bioactive lactose-modified chitosan: From synthesis to characterization. *Carbohydrate Polymers, 174*, 360–368.

Furlani, F., Sacco, P., Scognamiglio, F., Asaro, F., Travan, A., Borgogna, M., ... Donati, I. (2019). Nucleation, reorganization and disassembly of an active network from lactose-modified chitosan mimicking biological matrices. *Carbohydrate Polymers, 208*, 451–456.

Higashimura, M., Mulder-Bosman, B. W., Reich, R., Iwasaki, T., & Robijn, G. W. (2000). Solution properties of viilian, the exopolysaccharide from Lactococcus lactis subsp. Cremoris SBT 0495. *Biopolymers, 54*(2), 143–158.

Krishna Rao, K. S. V., Vijaya Kumar Naidu, B., Subha, M. C. S., Sairam, M., & Aminabhavi, T. M. (2006). Novel chitosan-based pH-sensitive interpenetrating network microgels for the controlled release of cefadroxil. *Carbohydrate Polymers, 66*(3), 333–344.

Li, F., Liu, W. G., & Yao, K. D. (2002). Preparation of oxidized glucose-crosslinked N-alkylated chitosan membrane and in vitro studies of pH-sensitive drug delivery behaviour. *Biomaterials, 23*(2), 343–347.

Matanović, M. R., Kristl, J., & Grabnar, P. A. (2014). Thermoresponsive polymers: Insights into decisive hydrogel characteristics, mechanisms of gelation, and promising biomedical applications. *International Journal of Pharmaceutics, 472*(1), 262–275.

Navarini, L., Abatangelo, A., Bertocchi, C., Conti, E., Bosco, M., & Picotti, F. (2001). Isolation and characterization of the exopolysaccharide produced by Streptococcus thermophilus SFi20. *International Journal of Biological Macromolecules, 28*(3), 219–226.

Prasad, K., Mondal, D., Sharma, M., Freire, M. G., Mukesh, C., & Bhatt, J. (2018). Stimuli responsive ion gels based on polysaccharides and other polymers prepared using ionic liquids and deep eutectic solvents. *Carbohydrate Polymers, 180*, 328–336.

Ren, Y., Zhao, X., Liang, X., Ma, P. X., & Guo, B. (2017). Injectable hydrogel based on quaternized chitosan, gelatin and dopamine as localized drug delivery system to treat Parkinson's disease. *International Journal of Biological Macromolecules, 105*, 1079–1087.

Ruel-Gariépy, E., Shive, M., Bichara, A., Berrada, M., Le Garrec, D., Chenite, A., & Leroux, J.-C. (2004). A thermosensitive chitosan-based hydrogel for the local delivery of paclitaxel. *European Journal of Pharmaceutics and Biopharmaceutics, 57*(1), 53–63.

Sacco, P., Cok, M., Asaro, F., Paoletti, S., & Donati, I. (2018). The role played by the molecular weight and acetylation degree in modulating the stiffness and elasticity of chitosan gels. *Carbohydrate Polymers, 196*, 405–413.

Sacco, P., Furlani, F., Cok, M., Travan, A., Borgogna, M., Marsich, E., ... Donati, I. (2017). Boric acid induced transient cross-links in lactose-modified chitosan (Chitlac). *Biomacromolecules, 18*(12), 4206–4213.

Sacco, P., Furlani, F., De Marzo, G., Marsich, E., Paoletti, S., & Donati, I. (2018). Concepts for Developing Physical Gels of Chitosan and of Chitosan Derivatives. *Gels, 4*(3), 67.

Sacco, P., Furlani, F., Paoletti, S., & Donati, I. (2019). pH-Assisted gelation of lactose-modified chitosan. *Biomacromolecules, 20*(8), 3070–3075. https://doi.org/10.1021/acs.biomac.9b00636.

Saravanan, S., Vimalraj, S., Thanikaivelan, P., Banudevi, S., & Manivasagam, G. (2019). A review on injectable chitosan/beta glycerophosphate hydrogels for bone tissue regeneration. *International Journal of Biological Macromolecules, 121*, 38–54.

Shanmugam, A., Kathiresan, K., & Nayak, L. (2016). Preparation, characterization and antibacterial activity of chitosan and phosphorylated chitosan from cuttlebone of Sepia kobiensis (Hoyle, 1885). *Biotechnology Reports, 9*, 25–30.

Shariatinia, Z. (2018). Carboxymethyl chitosan: Properties and biomedical applications. *International Journal of Biological Macromolecules, 120*, 1406–1419.

Tømmeraas, K., Köping-Höggård, M., Vårum, K. M., Christensen, B. E., Artursson, P., & Smidsrød, O. (2002). Preparation and characterisation of chitosans with oligosaccharide branches. *Carbohydrate Research, 337*(24), 2455–2462.

Ubaid, M., & Murtaza, G. (2018). Fabrication and characterization of genipin cross-linked chitosan/gelatin hydrogel for pH-sensitive, oral delivery of metformin with an application of response surface methodology. *International Journal of Biological Macromolecules, 114*, 1174–1185.

Vårum, K. M., & Smidsrød, O. (2004). Structure-property relationship in chitosans. In D. Severian (Ed.). *Polysaccharides: Structural diversity and functional versatility* (pp. 625–642). New York: CRC Press.

Wang, T., Zhou, Y., Xie, W., Chen, L., Zheng, H., & Fan, L. (2012). Preparation and anticoagulant activity of N-succinyl chitosan sulfates. *International Journal of Biological Macromolecules, 51*(5), 808–814.

Xu, S., Li, H., Ding, H., Fan, Z., Pi, P., Cheng, J., & Wen, X. (2019). Allylated chitosan-poly (N-isopropylacrylamide) hydrogel based on a functionalized double network for

controlled drug release. *Carbohydrate Polymers, 214*, 8–14.
Yong, H., Wang, X., Zhang, X., Liu, Y., Qin, Y., & Liu, J. (2019). Effects of anthocyanin-rich purple and black eggplant extracts on the physical, antioxidant and pH-sensitive properties of chitosan film. *Food Hydrocolloids, 94*, 93–104.
Zhang, W., Jin, X., Li, H., Zhang, R., & Wu, C. (2018). Injectable and body temperature sensitive hydrogels based on chitosan and hyaluronic acid for pH sensitive drug release. *Carbohydrate Polymers, 186*, 82–90.
Zhu, Y., Ma, Y., Zhao, Y., Yang, M., & Li, L. (2019). Preparation and evaluation of highly biocompatible nanogels with pH-sensitive charge-convertible capability based on doxorubicin prodrug. *Materials Science and Engineering C, 98*, 161–176.